

# Theoretical analysis of energy-dependent hot-electron transport in a magnetic multilayer

Takashi Yamauchi and Koichi Mizushima

*Advanced Materials and Devices Laboratory, Corporate Research and Development Center, Toshiba Corporation, Kawasaki, Kanagawa 210, Japan*

(Received 14 September 1999)

We analyzed the voltage dependence of the magnetoresistance (MR) ratio of a three-terminal device whose base consists of a magnetic multilayer. The spin-dependent current density of hot electrons in the base, which are injected from an emitter by tunneling, were calculated by using the Liouville equation for the spin-dependent Wigner distribution function. It was found to be necessary to take into account not only the spin dependence of elastic scattering but also the energy dependence of inelastic scattering and, furthermore, the forward-focusing effect of the Schottky barrier that exists at a base/collector interface, in order to understand the large MR ratio observed in this device and its monotonic decrease with increasing applied voltage.

## I. INTRODUCTION

Monsma *et al.*<sup>1</sup> and the present authors<sup>2,3</sup> proposed a three-terminal device where only hot electrons injected from an emitter into a magnetic multilayer in a base contribute to the collector current (hereafter, for simplicity, we call this a hot-electron device). In these works, the collector current was reported to change more than 200% under application of a magnetic field. Moreover, according to the experimental results in Ref. 2, the magnetoresistance (MR) ratio decreases monotonically over the voltage range from 1 to 1.8 V and the voltage dependence does not reflect the density of states (DOS) in the  $d$  bands in Fe. These experimental results are of great interest from both physical and practical points of view. In the analysis in Ref. 4, we divided the  $d$  bands into parabolic bands (free-electron-like bands of  $T_{2g}$  symmetry at  $\Gamma$ ) and narrow  $d$  bands, and calculated their contributions to the current density. We found that the current-voltage characteristics do not reflect the DOS in the  $d$  bands since electrons in the narrow  $d$  bands in the ferromagnetic layers are very likely to be scattered in the base due to their large effective mass and do not contribute to the current density. In this paper, we make a more quantitative comparison with the experimental results, by taking into account both spin and energy dependences of scatterings for electrons transporting in the parabolic bands. In order to compute the MR ratio of the hot-electron device, it is necessary to take into account the tunneling through the barrier at the emitter/base interface as well as the scattering in the base. We use one-dimensional Liouville equation for the Wigner distribution function<sup>5</sup> (WDF), which reduces to the Boltzmann equation<sup>6-10</sup> in the classical limit of  $\hbar \rightarrow 0$ .<sup>4,11,12</sup> This formalism has been used to study the one-dimensional quantum-based devices made of semiconductor layers.<sup>12-17</sup> However, we encounter difficulties as discussed below when we apply these WDF methods straightforwardly to the calculation of the current density in the hot-electron device. In Sec. II the reason that these difficulties occur in the numerical calculation by the WDF formalism is clarified and a method is proposed to avoid these difficulties. In Sec. III the calculation results are presented and the voltage dependence of the MR ratio for the hot-electron device is discussed.

## II. FORMULATION

### A. Modeling of the hot-electron device

In this section, we discuss the modeling of the hot-electron device.<sup>2</sup> In this device, only electrons with an energy higher than the Schottky barrier height  $eV_b$  [ $\sim 0.85$  eV (Ref. 2)] make a contribution to the collector current. In order to analyze the current-voltage characteristics in the actual device, it is necessary to take into account the band bending of the semiconductor collector, which is calculated by solving the transport equations with Poisson's equation self-consistently.<sup>18</sup> In this paper, to simplify the numerical calculation, we replaced the Schottky barrier at the base/collector interface by a tunneling barrier, as shown in Fig. 1. In the voltage range above  $\sim 1.5$  V, this model leads to results that are well fitted to the experimental results in Ref. 2 as discussed in Sec. III. Below  $\sim 1.5$  V, in contrast, the replacement of the Schottky barrier by the tunneling barrier causes considerable discrepancies between the results of experiment and calculation. This problem can be solved by taking into account, separately, the forward-focusing effect of the Schottky junction.

We used the one-dimensional Liouville equation for calculating the tunneling through the barrier and the scattering

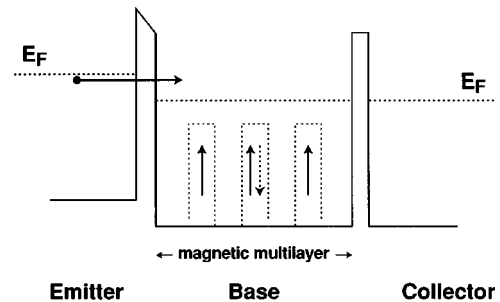


FIG. 1. Schematic energy diagram of the model that consists of the layers Au(55 Å)//Au(20 Å)/Fe(15 Å)/Au(15 Å)/Fe(15 Å)/Au(15 Å)/Fe(15 Å)/Au(20 Å)//Au(55 Å). The voltage is applied only across the tunneling barrier at the emitter/base interface and hot electrons are injected into a magnetic multilayer in the base. The horizontal dashed line in the base shows the bottom of the minority-spin band in Fe.

in the base simultaneously. In the calculation, it was noted that the discretization of the Liouville equation results in the violation of the principle of detailed balance.<sup>13</sup> In other words, we need to make the mesh spacings much finer in order to calculate the current density for an asymmetric structure than for a symmetric structure. Therefore, we performed the calculation for the case in which the number of Fe layers in the base is three, as shown in Fig. 1, because the structure of this model is symmetric both in the parallel and in the antiparallel configurations. We took the thickness of the layers as Au(55 Å)//Au(20 Å)/Fe(15 Å)/Au(15 Å)/Fe(15 Å)/Au(15 Å)/Fe(15 Å)/Au(20 Å)//Au (55 Å), respectively, where the double slash represents the tunnel barrier with a height of 1.5 eV and a width of 10 Å.

By calculating the current densities  $J_P$  and  $J_{AP}$  in the parallel (P) and in the antiparallel (AP) configurations respectively, we can obtain the MR ratio from the following equation:

$$\text{MR} = \frac{J_P - J_{AP}}{J_{AP}} \times 100\%. \quad (1)$$

Let us take the longitudinal direction as the  $x$  axis, and the Hamiltonian that represents the electron transport of the model in Fig. 1 is written as

$$H = -\frac{\hbar^2}{2m^*} \frac{d^2}{dx^2} + v(x) + h(x)\sigma, \quad (2)$$

where  $v(x)$  is the bottom of the conduction band and  $h(x)\sigma$  is the exchange energy at  $x$ , where  $h(x)$  is the molecular field in the Fe layer and  $\sigma$  ( $=1$  or  $0$ ) is the spin operator. This Hamiltonian is similar to what Slonczewski proposed for discussing the spin-polarized tunneling between the ferromagnetic films through a thin insulating barrier.<sup>54</sup> Furthermore, we can take the effective mass  $m^*$  as 1 at every point in the device, because the free-electron-like bands of  $T_{2g}$  symmetry at  $\Gamma$  ( $s$ -like bands) contribute dominantly to the electron conduction in the ferromagnetic layers.

The Liouville equation can be introduced from this Hamiltonian as follows:

$$\begin{aligned} \frac{\partial f_\sigma}{\partial t} &= -\frac{\hbar k_x}{m^*} \frac{\partial f_\sigma}{\partial x} - \frac{1}{\hbar} \int_{-\infty}^{\infty} \frac{dk'_x}{2\pi} V(x, k_x - k'_x) f_\sigma(x, k'_x) \\ &\equiv (\mathbf{L} \cdot \mathbf{f})_\sigma(x, k_x), \end{aligned} \quad (3)$$

$$\begin{aligned} V(x, k_x - k'_x) &= 2 \int_0^\infty dy [v(x + y/2) + h(x + y/2)\sigma \\ &\quad - v(x - y/2) - h(x - y/2)\sigma] \sin[(k_x - k'_x)y], \end{aligned}$$

where  $\mathbf{L}$  is called the Liouville superoperator.<sup>13</sup> We solved the Liouville equation (3) numerically, referring to the literature.<sup>13,18</sup> By substituting the WDF  $f_\sigma(x, k_x)$  obtained from Eq. (3) into the equations below, we can get the electron density and the current density. The electron density  $n(x)$  and the current density  $j(x)$  that are consistent with the Liouville equation (3) are represented by

$$n(x) = \sum_\sigma \int_{-\infty}^{\infty} \frac{dk_x}{2\pi} f_\sigma(x, k_x),$$

$$j(x) = \sum_\sigma \int_{-\infty}^{\infty} \frac{dk_x}{2\pi} \frac{\hbar k_x}{m^*} f_\sigma(x, k_x). \quad (4)$$

Here, we adapted the open-system boundary condition<sup>13</sup> to solve Eq. (3), and it is given by

$$\begin{aligned} f_{\sigma, \text{left}}^{k_x > 0} &= f_0(k_x), \\ f_{\sigma, \text{right}}^{k_x < 0} &= f_0(k_x), \\ f_0^*(k_x) &= \frac{1}{4\pi} (k_F^2 - k_x^2) \quad (|k_x| \leq k_F), \end{aligned} \quad (5)$$

where  $f_0^*$  is the Fermi-Dirac distribution function with the transverse momentum components integrated out, and in our model, we set the Au layers of the emitter and collector as reservoirs where the Fermi-Dirac distribution function is required.

## B. Tunneling current through the single barrier

The WDF formalism has been used in order to calculate the current-voltage characteristics of semiconductor devices, for instance, resonant tunneling diodes (RTD's), and the methods for the numerical calculation have been studied in many papers. However, it is difficult to apply these WDF methods directly to the numerical calculation of the current density of the hot-electron device, since the metal/insulator/metal tunnel junction in this device has much larger tunnel resistance than the semiconductor I/ semiconductor II/ semiconductor I tunnel junction. This problem has been pointed out by Jensen and Ganguly in their papers,<sup>19,20</sup> where a detailed comparison of the WDF approach was made with the Fowler-Nordheim approach<sup>21,22</sup> for the field emission from a metal into the vacuum. We propose a method to improve the accuracy of the WDF calculation of the tunneling current through the single barrier at the emitter/base interface.

We consider the following sequence of potential barriers  $v_\alpha$ :

$$v_\alpha(x) = \frac{h}{\Gamma(1 + 1/\alpha)} \exp\left[-\left(\frac{2|x|}{W}\right)^\alpha\right] \quad (\alpha \geq 1), \quad (6)$$

where  $h$  and  $W$  denote the height and the width of the tunnel barrier at the emitter/base interface, respectively. The coefficient of the right-hand side of Eq. (6) is a normalization factor. Figure 2 shows the energy diagrams for applying 1 V across the barriers in the cases for  $\alpha=2, 4$ , and  $\infty$ , respectively. It can be seen from this figure that  $v_\infty$  is the form of the abrupt potential barrier and that making  $\alpha$  small corresponds to smoothing out the potential barrier. In particular, when  $\alpha=2$ , we can calculate the potential term of the Liouville equation exactly and it is written as follows:

$$V(x, k_x) = 4hWe^{-k_x^2 W^2/4} \sin 2k_x x. \quad (7)$$

Here, we consider the following scale transformation:

$$\begin{aligned} \tilde{t} &= \bar{\tau}t, \\ \tilde{k}_x &= k_x/k_F, \end{aligned}$$

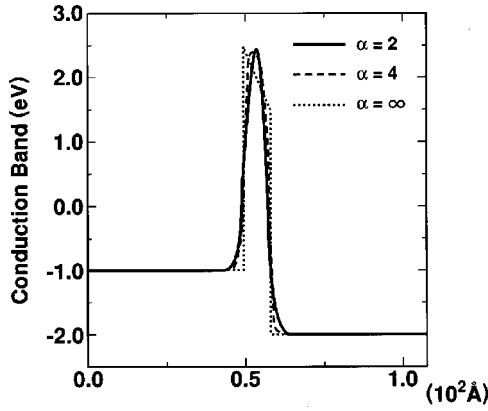


FIG. 2. Potential diagrams for applying 1 V across the barriers in the cases that  $\alpha=2,4,\infty$ . The interface of the barrier becomes smoother for smaller values of  $\alpha$ .

$$\begin{aligned}\tilde{\chi} &= k_F x, \\ \tilde{h} &= 4h/E_F, \\ \tilde{W} &= k_F W/2, \\ \tilde{\tau} &= 2E_F/\hbar.\end{aligned}\quad (8)$$

The Liouville equation (3) and the potential term (7) are transformed into

$$\begin{aligned}\frac{\partial \tilde{f}_\sigma}{\partial \tilde{t}} &= -\tilde{k}_x \frac{\partial \tilde{f}_\sigma}{\partial \tilde{x}} - \tilde{h} \int_{-\infty}^{\infty} \frac{d\tilde{k}'_x}{2\pi} \tilde{V}_{\tilde{W}}(\tilde{x}, \tilde{k}_x - \tilde{k}'_x) \tilde{f}_\sigma(\tilde{x}, \tilde{k}'_x), \\ \tilde{V}_{\tilde{W}}(\tilde{x}, \tilde{k}_x) &= \tilde{W} e^{-\tilde{W}^2 \tilde{k}_x^2} \sin 2\tilde{k}_x \tilde{x}, \\ \tilde{f}_\sigma(\tilde{x}, \tilde{k}_x) &= f_\sigma(\tilde{x}/k_F, k_F \tilde{k}_x)/k_F^2,\end{aligned}\quad (9)$$

and Eqs. (4) and (5) are also transformed into

$$\begin{aligned}n(\tilde{x}) &= k_F^3 \sum_{\sigma} \int_{-\infty}^{\infty} \frac{d\tilde{k}_x}{2\pi} \tilde{f}_\sigma(\tilde{x}, \tilde{k}_x), \\ j(\tilde{x}) &= k_F^4 \sum_{\sigma} \int_{-\infty}^{\infty} \frac{d\tilde{k}_x}{2\pi} \frac{\hbar \tilde{k}_x}{m^*} \tilde{f}_\sigma(\tilde{x}, \tilde{k}_x), \\ \tilde{f}_0^* &= \frac{1}{4\pi} (1 - \tilde{k}_x^2) \quad (|\tilde{k}_x| \leq 1).\end{aligned}\quad (10)$$

These equations imply that if two systems have the same values of  $\tilde{h}$  and  $\tilde{W}$ , the WDF  $f_\sigma(x, k_x)$  of each system is obtained from the same function  $\tilde{f}_\sigma$  defined on the phase space  $(\tilde{x}, \tilde{k}_x)$ . Roughly speaking, we can consider that systems with the same tunnel resistance are connected via this transformation (8). For example, the two systems with parameters  $E_F = 2$  eV,  $m^* = 1$ ,  $h = 3.5$  eV,  $W = 10$  Å and with those  $E'_F = 0.05$  eV,  $m^{*'} = 0.068$ ,  $h' = 0.0875$  eV,  $W' = 242$  Å have the same tunnel resistance. We have discussed the Liouville equation with the potential term (7), but it can

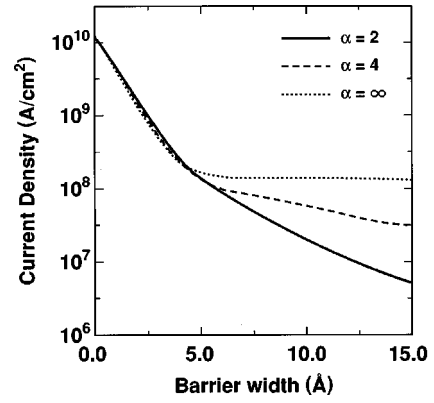


FIG. 3. This figure shows the current density through each barrier shown in Fig. 2 against its thickness.

be easily found that this transformation (8) is valid for the Liouville equation with the general potential term, moreover, including the collision term.

Next, we discuss the calculation results of the tunneling current through the single barrier at the emitter/base interface. The mesh spacing  $\Delta x'$  is taken as about a lattice constant ( $\sim 10$  Å) in the RTD simulation. Therefore, we determined the mesh spacing  $\Delta x$  in our model as  $0.41$  Å ( $= \Delta x' k_F / k'_F$ ), according to the above discussions. We took the cutoff of the Fourier transform in the Liouville equation (3) as  $2\pi/\Delta x$  and the number of discretization points in the longitudinal momentum space  $N_{k_x}$  as 300 and calculated the current density in the steady state ( $\partial f/\partial t = 0$ ). Shown in Fig. 3 is the current density at 1 V against the barrier width. The dotted line in this figure illustrates the calculation result in the case for  $\alpha = \infty$ . In this case, we find that the current density decreases as the barrier width increases and becomes nearly constant in the range of width larger than about 5 Å. However, the current density is considered to decrease monotonically even in this range, as shown by the stationary-state model.<sup>23,24</sup> Therefore, the results by the WDF method are not reliable in this range. The tunnel resistance of this insulating barrier can be found from Eq. (8) to correspond to that of the semiconductor barrier of 100 Å thickness. Therefore, we can consider that the calculation results by the WDF method are sufficiently reliable for RTD's with barriers of 30–60 Å thickness, even though those barriers are the rectangular barriers. In contrast, the calculation is not reliable in the case of the present device with rectangular barriers of 1.5 eV height and 10 Å thickness. One method to settle this problem may be making the mesh spacing  $\Delta x$  finer, although the CPU time is too large.

Alternatively, in this paper, we performed this calculation by smoothing out the potential barrier.<sup>19</sup> As seen in Fig. 3, the current density decreases with the barrier thickness more sensitively for a smaller value of  $\alpha$ . Therefore, we took the tunneling barriers both at the emitter/base and at the base/collector interfaces as the Gaussian potential barrier of Eq. (7) to improve the reliability of the calculation. The reason why smoothing out the potential barrier is of great advantage in the numerical calculation by the WDF formalism can be explained as follows. The Fourier transform of the rectangular potential  $v_\infty(x)$  is written as  $2 \sin(Wk_x/2)/k_x W$  and oscillates in the momentum space. Since the oscillation period

becomes shorter as the barrier width gets larger, we need to increase the number of grid points in the momentum space intensively. On the other hand, the Fourier transform of Gaussian potential is  $\exp[-(Wk_x/2)^2]$ , which changes monotonically in momentum space and is much easier to be handled in the form of a discrete Fourier transform.<sup>25</sup> Therefore, smoothing out the potential barrier enables us to perform a numerical calculation by the WDF formalism within a shorter CPU time and to make this calculation very stable. Moreover, we may consider that the potential barrier in the actual device is nearly Gaussian for the following two reasons: for rounding off the corners of the barrier by the image charge effect and for the spacial variation of the composition  $x$  of the  $\text{AlO}_x$  barrier fabricated by the oxidizing Al surface. Accordingly, we were willing to use this method in the WDF formalism.

### C. Collision term

The collision term in the one-dimensional Liouville equation (3) has been discussed in many papers.<sup>26–29</sup> It is usual to use the collision term in the relaxation-time approximation represented by

$$\left(\frac{\partial f}{\partial t}\right)_c = \frac{1}{\tau^*} \left( \frac{\int f(x, k_x)}{\int f_{\text{eq}}(x, k_x)} f_{\text{eq}}(x, k_x) - f(x, k_x) \right), \quad (12)$$

where  $f_{\text{eq}}(x, k_x)$  is given by the solution to  $\mathbf{L} \cdot \mathbf{f} = 0$  in the unbiased steady state. This collision term was introduced by Jensen and Buot<sup>27</sup> from the general form

$$\left(\frac{\partial f}{\partial t}\right)_c = \int_{-\infty}^{\infty} \frac{dk'_x}{2\pi} [W_{k'_x, k_x} f(x, k'_x) - W_{k_x, k'_x} f(x, k_x)], \quad (13)$$

under the assumptions that this equation satisfies the detailed balance condition and that the  $k_x$  dependence of  $W_{k'_x, k_x}$  is sufficiently small. The relaxation-time approximation has the advantage of combining some different scattering processes in one parameter  $\tau^*$ . Of course, the collision term (13) makes it possible for us to calculate the current-voltage characteristics by using a more realistic model of random scattering processes. However, we do not have a general method to obtain the transition rates  $W_{k'_x, k_x}$  from the three-dimensional transition rates  $W_{\mathbf{k}', \mathbf{k}}$  such that the collision term (13) does not violate the detailed balance condition.<sup>26,28</sup> Therefore, we used the collision term in the relaxation-time approximation of Eq. (12) in this work. The energy dependence of relaxation time cannot be taken into account in this term, since we have no information on the energy for a trajectory in the phase space  $(x, k_x)$ . Usually, we use the relaxation time that is averaged with respect to the energy according to

$$\tau^* = \int_0^{\infty} dE E^{3/2} f_0(E) \tau(E) / \int_0^{\infty} dE E^{3/2} f_0(E), \quad (14)$$

where  $f_0$  is the Fermi-Dirac distribution function.<sup>30</sup> However, in the hot-electron device, only electrons in the narrow energy range ( $\sim 0.5$  eV) near the Fermi level in the emitter are injected into the base due to the strong energy dependence of the tunneling probability for the electrons. There-

fore, it is not adequate to determine the mean relaxation time of injected electrons by using Eq. (14). Thus, we propose the following equation:

$$\tau^* = \int_0^{\infty} dE_x T(E_x) \int_0^{\infty} dE_t \tau(E_x + E_t) f_0(E_x + E_t) \times \left( \int_0^{\infty} dE_x T(E_x) \int_0^{\infty} dE_t f_0(E_x + E_t) \right)^{-1} \quad (15)$$

$$\equiv \langle T \rangle_E, \quad (16)$$

where  $T(E_x)$  is the transmission probability through the barrier at the emitter/base interface for an electron with energy  $E = E_x + E_t$ , which is calculated by the stationary-state model.<sup>23,24</sup> Since the denominator of Eq. (15) is proportional to the flux of electrons injected into the base from the emitter,<sup>31</sup> we can regard  $\tau^*$  as the mean relaxation time of electrons injected into the base.

### D. Elastic scattering

We may need to take into account a number of spin-dependent scattering processes for the entire understanding of the voltage dependence of the MR ratio detected in the hot-electron device.<sup>2</sup> In this paper, in particular, we took into account the elastic scattering by defects and the inelastic scattering by the Fermi sea, which were considered to be the principal influences on the electron transport in the base. In the case of the analysis of the CPP (current perpendicular to plane) MR, on the other hand, the effect of the spin-flip scatterings on the MR ratio has been studied in many papers, for example, the scattering by an impurity with a local moment,<sup>4,32–34</sup> by a magnon,<sup>35</sup> and by domain walls.<sup>36</sup> According to the experimental results,<sup>3,37,38</sup> the spin diffusion length is about two orders of magnitude larger than the mean free path for elastic scattering by defects and is much larger than the total thickness of the base layers of the hot-electron device. Therefore, we considered that the spin-flip scattering has a small influence on the voltage dependence of the MR ratio at voltages between 1 and 1.8 V in the experiment<sup>2</sup> and neglected the effect of the spin-flip scattering in this work.

The interaction with a defect is given by the screened Coulomb interaction:<sup>39</sup>

$$V(r) = \frac{-Ze^2}{4\pi\epsilon_0} \frac{e^{-|\mathbf{r}-\mathbf{r}_0|/\lambda_{\text{sc}}}}{|\mathbf{r}-\mathbf{r}_0|},$$

where  $\lambda_{\text{sc}}$ ,  $\epsilon_0$ , and  $Z$  are the screening length, the permittivity of vacuum, and the number of valence electrons in the metal, respectively. The relaxation time for an electron scattered by a defect in a free-electron-like metal is written as follows:

$$\tau_e^{s \rightarrow s}(E) = \frac{8\pi\hbar^3 \epsilon_0^2 k^3}{Ne^4 m^* Z^2} \left[ \ln(1 + 4\lambda_{\text{sc}}^2 k^2) - \frac{1}{1 + (4\lambda_{\text{sc}}^2 k^2)^{-1}} \right]^{-1},$$

$$E = \frac{\hbar^2 k^2}{2m^*}, \quad (17)$$

where  $N$  is the defect concentration.<sup>30</sup> However, we should consider that the relaxation time for an electron in the Fe

layer is spin dependent, according to Mott's transport theory.<sup>40,41</sup> That is, electrons transport mainly in the broad bands and the vacant narrow  $d$  bands act as final states of scattering of electrons scattered elastically or inelastically. Therefore, the relaxation time for a minority-spin electron reflects the DOS in the minority-spin band and is much smaller than that given by Eq. (17).

Let these transition rates from a  $s$  state to a  $d$  state be  $W_{s \rightarrow d}$ , and this collision term can be written as

$$\left(\frac{\partial f}{\partial t}\right)_C = \int_{-\infty}^{\infty} \frac{dk'_x}{2\pi} [W_{d \rightarrow s, k'_x, k_x} f(x, k'_x) - W_{s \rightarrow d, k_x, k'_x} f_d(x, k_x)], \quad (18)$$

where  $f_d$  denotes the distribution function of an electron in the  $d$  bands and the relaxation time  $\tau_e^{s \rightarrow d}$  is defined by

$$\frac{1}{\tau_e^{s \rightarrow d}} = \sum_{k'_x} W_{s \rightarrow d, k_x, k'_x}. \quad (19)$$

Here, noting that the energy of an electron is conserved in the process of elastic scattering, we may write Eq. (19) as

$$\frac{1}{\tau_e^{s \rightarrow d}(E)} \sim \frac{1}{\tau_e^{s \rightarrow s}(E)} \frac{D_{d\sigma}(E)}{D_s(E)}. \quad (20)$$

In addition, electrons in the narrow  $d$  bands, as already stated, do not contribute to the current. Thus, we can introduce the collision term in the relaxation-time approximation for  $s$ - $d$  scattering in the Fe layer as follows:

$$\left(\frac{\partial f}{\partial t}\right)_C = \frac{f(x, k_x) - f_{\text{eq}}(k, k_x)}{\tau_e^*}, \quad (21)$$

$$\tau_e^* = \left\langle \tau_e^{s \rightarrow s} \frac{D_s}{D_{d\sigma}} \right\rangle_E.$$

This collision term (21) represents that assumption that electrons scattered to a  $d$  state do not contribute to the current. Moreover, the mean relaxation time  $\tau_e^*$  in this term has strong voltage and spin dependences for electrons transporting in the Fe layer, since it reflects the DOS in the  $d$  bands. It is sufficient to take into account only  $s$ - $d$  scattering in the Fe layer, because it causes a much larger reduction of current density than  $s$ - $s$  scattering. Thus, we used the collision term (21) for the elastic scattering in the Fe layer and the collision term (12) for that in the Au layer.

### E. Inelastic scattering

We refer to the calculation results by Quinn and co-workers<sup>42-44</sup> regarding the relaxation time for inelastic scattering. They had derived the following formula from the imaginary part of the self-energy of an excited electron:

$$\frac{1}{\tau_i^{s \rightarrow s}(E)} = \frac{e^2}{\hbar \pi^2} \int_{E_F < E(\mathbf{k}-\mathbf{k}') < E(k)} \frac{d^3 \mathbf{k}'}{k'^2} \frac{\text{Im}[\epsilon(k', \Delta E)(\mathbf{k}')] }{|\epsilon(k', \Delta E(\mathbf{k}'))|^2} \quad (22)$$

$$\approx \frac{e^2}{\hbar a_0} \frac{\sqrt{\pi}}{32(\alpha r_s)^{1/2}} \left[ \tan^{-1} \left( \frac{\pi}{\alpha r_s} \right)^{1/2} + \frac{(\alpha r_s / \pi)^{1/2}}{1 + \alpha r_s / \pi} \right] \frac{[(k/k_F)^2 - 1]^2}{k/k_F},$$

$$\alpha \equiv \left( \frac{4}{9\pi} \right)^{1/3}, \quad (23)$$

where  $\epsilon(k', \Delta E(\mathbf{k}'))$  is the Lindhard dielectric constant<sup>45</sup> and  $k_F$ ,  $r_s$ , and  $a_0$  are the Fermi wave number, the Wigner-Seitz radius, and the Bohr radius, respectively. We took the Wigner-Seitz radius  $r_s$  in Au as 3, although, strictly speaking, Eq. (22) is justified in the random-phase approximation ( $r_s \approx 1$ ). By substituting this value of  $r_s$  into Eq. (22), we found that the individual particle collision is dominant for electrons with energy lower than 2 eV and that Eq. (22) is approximated by Eq. (23) in this energy range. Furthermore, we found that the mean free path is 200 Å at 1 eV and reduces to 70 Å in going from 1 to 2 eV. Regarding the lifetime of a hot electron transporting in the Fe layer, the  $s$ - $d$  transition is the most important factor that causes strong inelastic scattering and its spin dependence. We represented the relaxation time for inelastic scattering by modifying Eq. (20). Since the final states of inelastic scattering have the energy range  $\Delta E$  [ $\approx \hbar / \tau_i^{s \rightarrow s}(E)$ ], we averaged  $D_{d\sigma}(E)/D_s(E)$  over the range  $\Delta E$ . Thus, we can write the relaxation time for inelastic scattering as

$$\frac{1}{\tau_i(E)} = \frac{1}{\tau_i^{s \rightarrow s}(E)} \left\langle \frac{D_{d\sigma}(E)}{D_s(E)} \right\rangle_{\Delta E} + \frac{1}{\tau_i^{s \rightarrow s}(E)}, \quad (24)$$

where  $\langle \dots \rangle_{\Delta E}$  denotes averaging over the energy range of final states of scattering  $\Delta E$ . The averaging makes the reflection of the energy dependence of the DOS in the relaxation time smaller, and therefore the spin dependence of inelastic scattering becomes weaker than that of elastic scattering. In fact, the lifetime of hot electrons in fcc cobalt measured by a two-photon photoemission technique<sup>46</sup> shows weak spin dependence.<sup>47</sup>

Here, we should remark that electrons scattered inelastically either to an  $s$  state or to a  $d$  state flow out from the base due to the reflection at the Schottky barrier at the base/collector interface. Therefore, we need to use the collision term (21) for inelastic scattering and it is given by

$$\left(\frac{\partial f}{\partial t}\right)_C = \frac{f(x, k_x) - f_{\text{eq}}(x, k_x)}{\tau_i^*},$$

$$\tau_i^* = \langle \tau_i \rangle_E. \quad (25)$$

## III. RESULTS AND DISCUSSIONS

### A. The mean relaxation time

We analytically represented the DOS in the  $d$  bands in Fe (Ref. 48) by using the Lorentzian<sup>4,34</sup> as follows:

$$D_{d\sigma}(E) = \frac{5\alpha}{\pi a^3} \frac{\Delta}{(E - \bar{E}_\sigma)^2 + \Delta^2}, \quad (26)$$

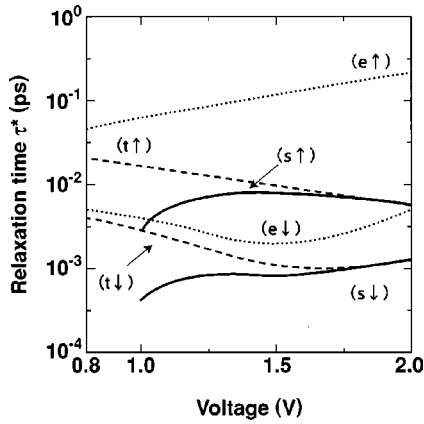


FIG. 4. The voltage dependence of the mean relaxation time of electrons injected from the emitter and transporting in the Fe layer.  $\uparrow$  and  $\downarrow$  show the spin directions of a majority- and minority-spin electron, respectively.

where  $\bar{E}_\uparrow$ ,  $\bar{E}_\downarrow$ ,  $E_F$ ,  $h\sigma$ , and  $\Delta$  are 1.2, 1.4, 2.5, and 0.4 eV, respectively, the number of atoms in the unit cell  $\alpha$  is 2 for bcc, and the lattice constant  $a$  is 2.867 Å. The DOS in Au for energy  $E$ , taking it as a free-electron-like metal, is written as

$$D_s(E) = \frac{3}{2} \frac{\alpha}{a^3} \frac{\sqrt{E}}{E_F^{2/3}}, \quad (27)$$

where  $E_F$  is 2 eV,  $\alpha$  is 4 for fcc, and  $a$  is 4.079 Å.

In Fig. 4 the mean relaxation time  $\tau^*$  for an electron transporting in the Fe layer is shown as a function of bias voltage applying between the emitter and the base. The dotted line indicates the mean relaxation time for elastic scattering with 0.5% defect and the dashed line indicates the total relaxation time  $\tau_t^* = (1/\tau_e^* + 1/\tau_i^*)^{-1}$  (Matthiessen's rule<sup>30</sup>). We found from this figure that  $\tau_e^*$  reflects the DOS in the  $d$  bands and that a minimum exists for a minority-spin electron at the voltage ( $\sim 1.5$  V) corresponding to the peak of the minority-spin bands in Fe. However, including the inelastic scattering, this minimum does not appear clearly, because the inelastic scattering with a weak spin dependence is dominant in the higher-voltage region.

### B. Calculation results of the MR ratio

Next, we calculated the MR ratio of the model in Fig. 1. We took  $N_{k_x}$  as 360 for solving the Liouville equation (3). First, we studied the dependence of the current density on the strength of elastic scattering that was changed by the uniform concentration in the base layers. The results of these calculation are shown in Fig. 5. As the defect concentration increases, the difference between configurations was found to become large. Taking the defect concentration as 0.5%, we calculated the voltage dependence of the MR ratio. As illustrated by the dotted line in Fig. 6, the voltage dependence of the MR ratio reflects the DOS in the  $d$  bands in the Fe layers, and a maximum exists at about 1.5 V corresponding to the peak in the minority-spin band. As shown by the dashed line, the inclusion of inelastic scattering smooths out this peak and the MR ratio decreases slowly with voltage in a range higher than 1.5 V. This voltage dependence is ascribed to that of the mean relaxation time shown in Fig. 4. Therefore, we can

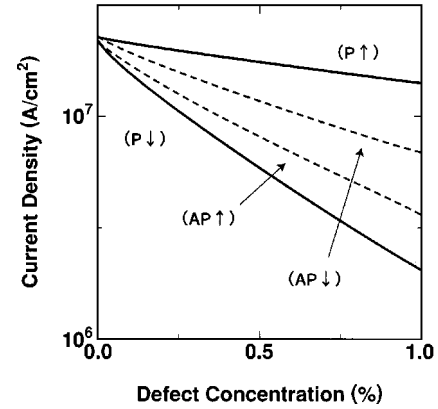


FIG. 5. This figure shows the current density through the model shown in Fig. 1 at 1 V as a function of defect concentration in the base layers.  $\uparrow$  and  $\downarrow$  mean the same as those in Fig. 4. The symbols P and AP denote the parallel and antiparallel configurations, respectively.

conclude that inelastic scattering affects the voltage dependence of the MR ratio considerably at voltages above 1.5 V. At voltages below 1.5 V, however, the MR ratio increases monotonically with the voltage, and this result is different from the experimental result.<sup>2</sup> This discrepancy is caused by the forward-focusing effect of the Schottky barrier, which has not been taken into account in our calculation as discussed below.

### C. Forward-focusing effect of the Schottky barrier

For a hot electron to flow into the collector its energy must be above  $eV_b$  and thereby its trajectory is limited to within the critical angle  $\theta_c$  to the normal of the Au/Si interface, as discussed in Ref. 2. Therefore, hot electrons scattered in the base are unlikely to flow into the collector. In other words, we can consider that the scattering in the base is enhanced by the forward-focusing effect of the Schottky barrier at the base/collector interface and the mean relaxation times should be shorter than those calculated by Eq. (15). This critical angle  $\theta_c$  is estimated to be  $15^\circ$  for an electron with energy 1 eV and naturally  $0^\circ$  for an electron with energy lower than the Schottky barrier height. It is necessary to use the three-dimensional model in order to discuss this effect rigidly. In this work, we propose a simple method to take into account this effect in the one-dimensional transport model. That is, we took  $\tau(E_x + E_t)$  as 0 for  $E_x \leq eV_b$  in Eq.

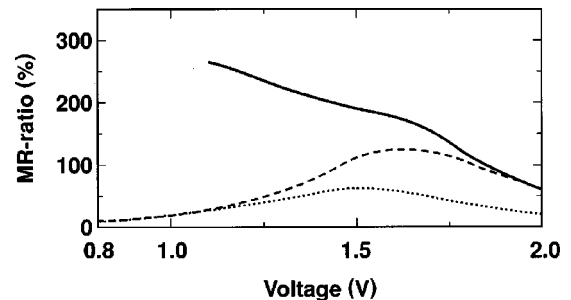


FIG. 6. The voltage dependence of the MR ratio. The data plotted in each line were calculated by using the mean relaxation times shown by the same line in Fig. 4.

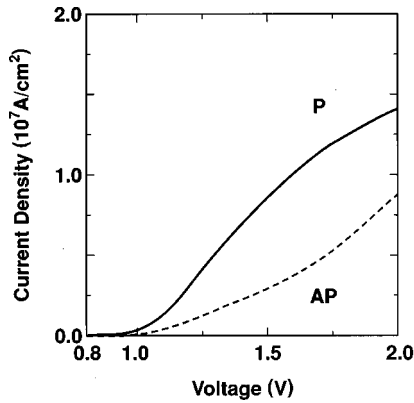


FIG. 7. The current-voltage characteristics obtained from the Liouville equation with the collision term including  $\tau_s^*$ . The symbols P and AP mean the same as those in Fig. 5.

(15) with the meaning that hot electrons with energy  $E$  ( $=E_x + E_t$ ) cannot flow into the collector if they reach the base/collector interface outside the angle  $\theta_c = \tan^{-1} \sqrt{(E - eV_b)/eV_b}$  to the normal of the base/collector interface. The calculation results of the mean relaxation time  $\tau_s^*$  by using this method are indicated by the solid line in Fig. 4. As seen in this figure,  $\tau_s^*$  is smaller than  $\tau_t^*$  at the voltages below 1.5 V, and this difference between  $\tau_s^*$  and  $\tau_t^*$  is larger as the voltage is lower. The voltage dependence of the MR ratio is indicated by the solid line in Fig. 6 and the current-voltage characteristics in Fig. 7. We found from Fig. 6 that the forward-focusing effect of the Schottky barrier modifies the voltage-dependence of the MR ratio in the range lower than 1.5 V and can account for the large MR ratio observed in this region. Moreover, as seen in Fig. 7, the current increases almost linearly with voltage between 1.1 and 1.5 V, as is observed in the experiment.<sup>2</sup>

#### IV. CONCLUSIONS

The authors reported on the voltage dependence of the MR ratio of the hot-electron device.<sup>2</sup> The following two results in this experiment should be noted. The first is that an MR ratio several times larger than the CPP MR was observed at voltages around 1 V. The second is that the MR ratio decreased monotonically over the voltage range in the experiment and that no anomaly was observed at the voltage ( $\sim 1.5$  V) corresponding to the peak in the DOS of the minority-spin bands in Fe. The purpose of this work is to explain these experimental results theoretically by using the model shown in Fig. 1. Since we need to take into account

the tunneling through the barriers for a hot electron, including the scattering events in the base, we used the WDF formalism. Based on the calculation results in the previous paper,<sup>4</sup> we postulated the Liouville equation for an electron transporting in the free-electron-like bands in the base layers. Namely, electrons in the narrow  $d$  bands do not contribute to the electron conduction in the Fe layer in our model. However, the vacant narrow  $d$  bands act as final states of scattering in the ferromagnetic layer, according to the Mott's transport theory.<sup>40,41</sup> Taking this effect into account, we studied the electron transport in the base. In particular, we pointed out the importance of both the elastic scattering by defects and the inelastic scattering in the Fe layer. From the calculation results of the voltage dependence of the MR ratio, we arrived at the following two conclusions:

(1) The spin dependence of the total relaxation time becomes weak in the region of voltage over 1.5 V, since the influence of inelastic scattering becomes strong. This leads to the result that the voltage dependence of the MR ratio does not reflect the DOS in Fe.

(2) Particular importance should be accorded to electron refraction with a small critical angle (forward-focusing effect) at the base/collector interface. The elastic scattering enhanced by this effect produces a large MR ratio detected at the voltage around 1 V.

We succeeded in explaining the experimental results by taking into account both spin and energy dependences of scatterings in the base of our model. However, for better fitting, it may be necessary to discuss the relaxation time for the  $s$ - $d$  scattering in the ferromagnetic layer more rigorously. For example, if we use the self-consistent Born approximation in this calculation,  $\Delta$  in the form of the DOS in the  $d$  bands, Eq. (26), may be found to be larger due to the influence of inelastic scattering. This effect can also contribute to the monotonic decrease of the MR ratio.

Although we did not discuss the tunnel magnetoresistance (TMR) in ferromagnetic junction,<sup>49,50</sup> which has also attracted much interest since the discovery of the quite large TMR,<sup>51,52</sup> our formalism can be applied to the calculation. Many models have already been proposed to obtain physical insights into this phenomenon,<sup>49,53-55</sup> but our formalism in this work may also be useful for the study of the TMR device, for example, the influences of scattering by a magnon and diffuse scattering on the TMR.

#### ACKNOWLEDGMENT

One of the authors (T.Y.) would like to thank Dr. K. Satoh of Medical Systems Company, Toshiba Corporation for fruitful discussions.

<sup>1</sup>D. J. Monsma, J. C. Lodder, J. A. Popma, and B. Dieny, Phys. Rev. Lett. **74**, 5260 (1995).

<sup>2</sup>K. Mizushima, T. Kinno, K. Tanaka, and T. Yamauchi, IEEE Trans. Magn. **33**, 3500 (1997).

<sup>3</sup>K. Mizushima, T. Kinno, K. Tanaka, and T. Yamauchi, Phys. Rev. B **58**, 4660 (1998).

<sup>4</sup>T. Yamauchi and K. Mizushima, Phys. Rev. B **58**, 1934 (1998).

<sup>5</sup>E. Wigner, Phys. Rev. **40**, 749 (1932).

<sup>6</sup>S. Zhang and P. M. Levy, J. Appl. Phys. **69**, 4786 (1991).

<sup>7</sup>E. Yu. Tsymbal and D. G. Pettifor, J. Phys.: Condens. Matter **8**, L569 (1996).

<sup>8</sup>T. Valet and A. Fert, Phys. Rev. B **48**, 7099 (1993).

<sup>9</sup>A. Fert and S.-F. Lee, Phys. Rev. B **53**, 6554 (1996).

<sup>10</sup>S. Y. Hsu, A. Barthélémy, P. Holody, R. Loloee, P. A. Schroeder, and A. Fert, Phys. Rev. Lett. **78**, 2652 (1997).

<sup>11</sup>G. J. Infrate, H. L. Grubin, and D. K. Ferry, J. Phys. (Paris),

- Colloq. **42**, C7-307 (1981).
- <sup>12</sup>H. Tsuchiya, M. Ogawa, and T. Miyoshi, IEEE Trans. Electron Devices **ED-38**, 1246 (1991).
- <sup>13</sup>W. R. Frensley, Rev. Mod. Phys. **62**, 745 (1990).
- <sup>14</sup>F. A. Buot, Phys. Rep. **234**, 73 (1993).
- <sup>15</sup>F. A. Buot and K. L. Jensen, Phys. Rev. B **42**, 9429 (1990).
- <sup>16</sup>K. L. Jensen and F. A. Buot, IEEE Trans. Electron Devices **38**, 2337 (1991).
- <sup>17</sup>K. L. Jensen and F. A. Buot, J. Appl. Phys. **65**, 5248 (1989).
- <sup>18</sup>M. Kurata, *Numerical Analysis for Semiconductor Devices* (Heath, Lexington, 1982).
- <sup>19</sup>K. L. Jensen and A. K. Ganguly, J. Appl. Phys. **73**, 4409 (1993).
- <sup>20</sup>K. L. Jensen and A. K. Ganguly, J. Vac. Sci. Technol. B **11**, 371 (1993).
- <sup>21</sup>R. H. Fowler and L. W. Nordheim, Proc. R. Soc. London, Ser. A **119**, 173 (1928).
- <sup>22</sup>L. W. Nordheim, Proc. R. Soc. London **121**, 626 (1928).
- <sup>23</sup>K. H. Gundlach, Solid-State Electron. **9**, 949 (1996).
- <sup>24</sup>Y. Ando and T. Itoh, J. Appl. Phys. **61**, 1469 (1987).
- <sup>25</sup>O. Brigham, *The Fast Fourier Transform* (Prentice-Hall, Englewood Cliffs, NJ, 1974).
- <sup>26</sup>W. R. Frensley, Solid-State Electron. **31**, 739 (1988).
- <sup>27</sup>K. L. Jensen and F. A. Buot, J. Appl. Phys. **67**, 7602 (1990).
- <sup>28</sup>J. García-García, X. Oriols, F. Martín, and J. Suñé, Solid-State Electron. **39**, 1795 (1996).
- <sup>29</sup>J. Lin and L. C. Chiu, J. Appl. Phys. **57**, 1973 (1985).
- <sup>30</sup>B. R. Nag, *Electron Transport in Compound Semiconductors* (Springer, Berlin, 1991).
- <sup>31</sup>R. Tsu and L. Esaki, Appl. Phys. Lett. **22**, 562 (1973).
- <sup>32</sup>Y. Yafet, J. Appl. Phys. **39**, 853 (1968).
- <sup>33</sup>Y. Yafet, J. Appl. Phys. **42**, 1564 (1971).
- <sup>34</sup>K. Yoshida, *Theory of Magnetism* (Springer, Berlin, 1996).
- <sup>35</sup>S. Zhang, P. M. Levy, A. C. Marley, and S. S. P. Parkin, Phys. Rev. B **79**, 3744 (1997).
- <sup>36</sup>S. Zhang and P. M. Levy, Phys. Rev. B **50**, 6089 (1994).
- <sup>37</sup>S.-Y. Hsu, P. Holody, R. Loloee, J. M. Ritter, W. P. Pratt, Jr., and P. A. Schroeder, Phys. Rev. B **54**, 9027 (1996).
- <sup>38</sup>P. Monod and S. Shultz, J. Phys. (France) **43**, 393 (1982).
- <sup>39</sup>J. M. Ziman, *Principles of the Theory of Solids* (Cambridge University Press, Cambridge, 1972).
- <sup>40</sup>N. F. Mott, *The Theory of the Properties of Metals and Alloys* (Dover, New York, 1958).
- <sup>41</sup>N. F. Mott, Proc. R. Soc. London, Ser. A **153**, 669 (1936).
- <sup>42</sup>J. J. Quinn and R. A. Ferrell, Phys. Rev. **112**, 812 (1958).
- <sup>43</sup>J. J. Quinn, Phys. Rev. **126**, 1453 (1962).
- <sup>44</sup>D. Pines, *Elementary Excitations in Solids* (Benjamin, New York, 1964).
- <sup>45</sup>J. Lindhard, K. Dan. Vidensk. Selsk. Mat. Fys. Medd. **28**, 8 (1954).
- <sup>46</sup>M. Aeschlimann, M. Bauer, S. Pawlik, W. Weber, R. Burgermeister, D. Oberli, and H. C. Siegmann, Phys. Rev. Lett. **79**, 5158 (1997).
- <sup>47</sup>G. Schönhense and H. C. Siegmann, Ann. Phys. (Leipzig) **2**, 465 (1996).
- <sup>48</sup>D. A. Papaconstantopoulos, *Handbook of the Band Structure of Elemental Solids* (Plenum, New York, 1986).
- <sup>49</sup>M. Jullière, Phys. Lett. **54A**, 225 (1975).
- <sup>50</sup>S. Maekawa and U. Gafvert, IEEE Trans. Magn. **18**, 707 (1982).
- <sup>51</sup>T. Miyazaki and N. Tezuka, J. Magn. Magn. Mater. **139**, L231 (1995).
- <sup>52</sup>J. S. Moodera, L. R. Kinder, T. M. Wong, and R. Meservey, Phys. Rev. Lett. **74**, 3273 (1995).
- <sup>53</sup>M. B. Stearns, J. Magn. Magn. Mater. **5**, 167 (1977).
- <sup>54</sup>J. C. Slonczewski, Phys. Rev. B **39**, 6995 (1989).
- <sup>55</sup>E. Yu. Tsymlal and D. G. Pettifor, Phys. Rev. B **58**, 432 (1998).